THE AMERICAN SOCIETY OF MECHANICAL ENGINEERS
345 E. 47 St., New York, N.Y. 10017

89-GT-150

An Experimental Investigation of Heat Transfer Coefficients in a Spanwise Rotating Channel with Two Opposite Rib-Roughened Walls

M. E. TASLIM and A. RAHMAN
Mechanical Engineering Department
Northeastern University
Boston, MA 02115

and

S. D. SPRING
Aircraft Engine Business Group
General Electric Company
Lynn, MA 01910

ABSTRACT

Liquid crystals are used in this experimental investigation to measure the heat transfer coefficient in a spanwise rotating channel with two opposite rib-roughened walls. The ribs (also called turbulence promoters or turbulators) are configured in a staggered arrangement with an angle of attack to the mainstream flow, α, of 90° for all cases. Results are presented for three values of turbulator blockage ratio, e/D_h (0.1333, 0.25, 0.333) and for a range of Reynolds numbers from 15,000 to 50,000 while the test section is rotated at different speeds to give Rotational Reynolds numbers between 450 and 1800. The Rossby number range is 10 to 100 (Rotation number of 0.1 to 0.01). The effect of turbulator blockage ratios on heat transfer enhancement is also investigated. Comparisons are made between the results of geometrically identical stationary and rotating passages of otherwise similar operating conditions. The results indicate that a significant enhancement in heat transfer is achieved in both the stationary and rotating cases, when the surfaces are roughened with turbulators. For the rotating case, a maximum increase over that of the stationary case of about 45% in the heat transfer coefficient is seen for a blockage ratio of 0.133 on the trailing surface in the direction of rotation and the minimum is a decrease of about 6% for a blockage ratio of 0.333 on the leading surface, for the range of rotation numbers tested. The technique of using liquid crystals to determine heat transfer coefficients in this investigation proved to be an effective and accurate method especially for nonstationary test sections.

NOMENCLATURE

a	test section width (see figure 2)
A_h	heat transfer area
AR	aspect ratio of passage, a/b
b	test section height
d	distance of camera lens from the beginning of the heater on which h_t is measured in the direction of flow
D	diameter of a circular passage
D_h	hydraulic diameter of passage, 2ab/(a+b)
e	turbulator (rib) height
h_t	heat transfer coefficient on turbulated wall
Gr	Grashof number $(=Ra/Pr = (\frac{r}{D_h})J_{D_h} Ro Re \beta \Delta T)$
i_k	current drawn by kth heater
J_D	Rotational Reynolds number based on circular tube diameter $= \Omega D^2/\nu$
J_{D_h}	Rotational Reynolds number based on hydraulic diameter $= \Omega {D_h}^2/\nu$
k	thermal conductivity of air
L	length of each heater in flow direction ($27.95cm$)
$\dot{m}$	mass flow rate of air
Nu_s	Nusselt number on the turbulated wall of the test section when the passage is stationary
Nu_r	Nusselt number on the turbulated wall of the test section when the passage is rotating
P	perimeter

Presented at the Gas Turbine and Aeroengine Congress and Exposition—June 4-8, 1989—Toronto, Ontario, Canada
This paper has been accepted for publication in the Transactions of the ASME
Discussion of it will be accepted at ASME Headquarters until September 30, 1989

Pr	Prandtl number
$\dot{q}''$	heat flux generated by electric heater
$\dot{q}''_b$	heat flux lost through back of test section
$\dot{q}''_r$	heat flux lost by radiation
$\dot{Q}$	total heat added to air
r	radial distance from the camera lens to the axis of rotation
Ra	Rotational Rayleigh number $(= r\Omega^2(T_w - T_m)\beta D_h^3 Pr/\nu^2$ $=(\frac{r}{D_h})J_{D_h} RoRePr\beta\Delta T)$
Re	Reynolds number based on test section hydraulic diameter
Ro	Rotation number $(=\Omega D_h/U_m)$
$Ross$	Rossby number $(=1/Ro)$
S	turbulator (rib) pitch
T	temperature
T_f	film temperature
T_m	air mixed mean temperature
T_w	wall surface temperature
U_m	mean velocity of air
V_k	voltage across kth heater
X'	non-dimensional distance between two turbulators
α	angle of attack
β	volumetric coefficient of thermal expansion
ν	kinematic viscosity of air
ρ	density
Ω	angular velocity
ΔT	$(T_w - T_m)$

INTRODUCTION

In modern gas turbine airfoil designs, operating in the presence of high turbine inlet temperatures, effective blade cooling is a necessity. As the need increases for these airfoils to operate in a higher temperature environment, the need for more effective blade cooling becomes critical. The heat transfer from the blade surface to the internal cooling air is considerably enhanced when the internal passages are roughened with turbulence promoters (ribs or turbulators) located at discrete positions along the passage wall. Geometric parameters such as passage aspect ratio (AR), turbulator height to passage hydraulic diameter or blockage ratio (e/D_h) , turbulator pitch-to-height ratio (S/e), turbulator angle of attack (α) and the manner in which the turbulators are positioned with respect to each other have pronounced effects on both local and overall heat transfer coefficients. Turbulators of different blockage ratios positioned at different angles of attack are presently used in advanced aircraft engines.

Experimental results for the stationary case have been widely reported for a variety of geometric variations. The interested reader is referred to work done by Burgraff (1970), Metzger et al. (1983), Han (1984), Han et al. (1978, 1985) and Taslim and Spring (1987, 1988). However, in actual operating conditions, the blade is rotated at high speeds. Hence, the coolant air experiences Coriolis and centripetal forces which affect the heat transfer to a considerable extent. Results of several investigations have been reported for rotating passages with smooth walls. Mori et al. (1971) presented a theoretical as well as experimental analysis for both laminar and turbulent flows in a rotating circular pipe. Johnston et al. (1972) showed that the effect of rotation on fully developed flow in a rectangular channel was to change the structure of turbulence near the leading and trailing walls. They used water as the working fluid, with dye for visualization and tested a Reynolds number range of 2,500 to 36,000 while the Rotation number was varied from 0.01 to 0.25. Lokai and Limanski (1975) conducted a series of experiments with radially outward flow for a heated circular tube with turbulent conditions. These authors noted improved heat transfer and proposed a correlation. Zysina-Molozhen et al. (1977) undertook a program of experiments with a radially outward flow and suggested that the flow tends to exhibit a more laminar-like behavior when rotation is present and at the higher end of their Reynolds number range ($Re \geq 2.5 \times 10^4$) , rotation has no serious effect. Mityakov et al. (1978) measured local and average effects of rotation on turbulent heat transfer in a circular tube rotating in an orthogonal mode. While maintaining a constant heat flux boundary condition, they reported results for a Reynolds number range of 5,500 to 50,000 while Rossby number was varied from 14 to 50. Morris and Ayhan (1979) presented results of an experimental investigation of rotational effects showing changes in the average Nusselt numbers to be of the order of ± 30% due to rotation. In their case, Reynolds number was varied from 5,000 to 15,000 and three rotational speeds of 0, 1000 and 2000 revolutions per minute were tested. In a later paper (1981) they examined radially inward flows and centripetal buoyancy effects, and concluded that centripetal buoyancy adversely affects heat transfer relative to

a stationary case when the flow is radially outwards. Data was presented showing the converse for radially inward flow. They suggested that Coriolis acceleration improves heat transfer for radially outward flow with converse conditions for inward flow. Wagner et al. (1986) performed experiments with typical airfoil internal cooling passages. They tested two models, a two pass model (one radially outward flow channel connected with a 180° bend to a radially inward channel) and an actual engine scale model. In the two pass model, the aspect ratio of the channels was 0.25. Experiments were conducted at rotational speeds up to 700 rpm for Reynolds numbers of 15,000 and 30,000. The model pressure was 10 atmospheres. The scaled engine model coolant passages were tested over a Rotation number range of 0 to 0.09. They concluded that the average heat transfer coefficients on the leading and trailing surfaces can be significantly increased or decreased depending upon flow direction and magnitude of Rossby number. Further, they suggested that the shape and orientation of the coolant passage can be expected to affect the heat transfer. Morris and Harasagama (1987) reported on the influence of Coriolis induced secondary flow within typical cooling passages. They experimented with square, triangular and circular sectioned passages over a Reynolds number range of 7,000 to 25,000 and rotational Reynolds number (defined as $\Omega D^2/\nu$) ranging from 100 to 1,000. They concluded that for a radially inward flow, mean Nusselt numbers with rotation generally tend to be higher than the corresponding zero speed case and as rotational Reynolds number increases, heat transfer on the leading side decreases. For radially outward flow, rotation caused a reduction in mean Nusselt number on the leading side with respect to zero speed comparisons. The heat transfer coefficient was higher on the trailing side than on the leading side, which they attributed to secondary flow effects, and as rotational speeds increased, mean Nusselt number increased.

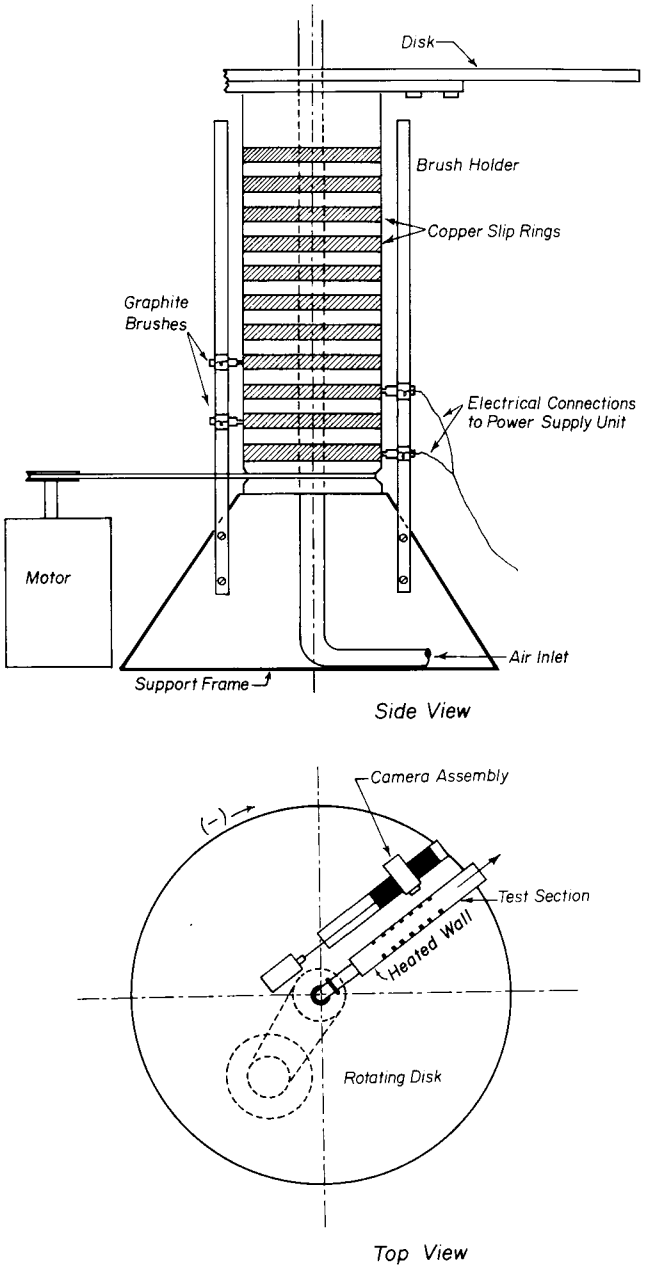

Fig. 1 Experimental apparatus

The objective of the experimental investigation reported upon in this paper is to measure the heat transfer coefficient in a spanwise rotating cooling passage roughened with turbulators of different geometries. Two opposite walls are turbulated in a staggered arrangement. Emphasis is put on the influence of Coriolis forces on internal heat transfer. Results are reported for three blockage ratios, 0.133, 0.250 and 0.333. The Rotation number varies between 0.01 to 0.1 and the Reynolds number is in the range of 15,000 to 50,000. The Rotational Reynolds number varies from 450 to 1800. The liquid crystal technique is used for temperature measurement.

EXPERIMENTAL APPARATUS

A schematic representation of the rotating test rig is shown in Fig 1. The plenum, test section and camera assembly are mounted on a light-weight circular disk of 2.44 m in diameter. A 3.6 KW dc motor rotates the disk. Air is supplied to the test rig through two filters and measured via a custom-made critical flow venturi, then enters the plenum and test section through a rotary joint. The

air, which is now at about ambient pressure and temperature, flows through a honeycomb type flow straightener located in the plenum and enters the test section through a bellmouth opening.

Three test sections are used, one for each size of turbulator. The test section length in the direction of flow is 116.84 cm and has a cross sectional area of 3.81 x 3.81 cm. Thus, the aspect ratio in each case is 1 and the hydraulic diameter is 3.81 cm. Figure 2 shows the layout of a typical test section. Three walls are made of 1.27-cm-thick clear plexiglass and the fourth is made of 1.06-cm-thick white pinewood. Turbulators are placed in a staggered arrangement on two opposite sides, one of which forms the heated wall on which measurements are taken. For the three test sections, the location of the first turbulator from the test section inlet is 40.6, 43.8 and 40.6 cm depending on the turbulator height. Others are placed consistent with keeping S/e=10, constant for all three sizes of turbulators (e= 5.08, 9.53 and 12.7 mm). The turbulators are glued into grooves machined in the plexiglass sides. They are also made of clear plexiglass with a square cross section equal to e and of length equal to passage side, 3.81 cm. The plexiglass walls and turbulators are glued and bolted together as one piece and then bolted onto the wooden wall, on which the liquid crystal sheet is attached and all measurements are taken. The wooden wall is 7.6-cm-wide and has the same length as the passage.

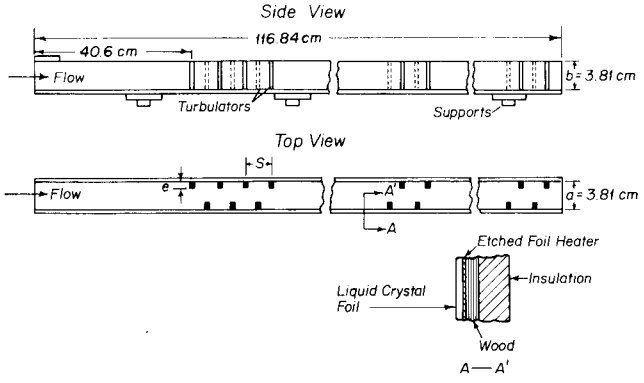

Fig. 2 Layout of a typical test section

It sits snugly against the plexiglass sides and turbulators to complete the passage.

Four custom-made etched foil heaters are placed on the wooden wall using a special double-stick 0.05-mm-thick tape with minimal temperature deformation. The heaters are each 27.95-cm-long and 3.81-cm-wide and cover the entire test section length including the non-turbulated entry length. However, they do not extend over the actual turbulator surface. Details of heater materials and arrangement are found in Rahman (1988). The liquid crystal sheet is placed on the heaters. The thickness of the liquid crystal layer is 0.15 mm.

The test section is covered on all sides, except for a small window at the location where the pictures are taken, by 5-cm-thick styrofoam sheets to minimize heat losses to the environment. A 35-mm, programmable camera is mounted on a platform which can travel along the length of the test section. The camera location is altered by activating a 50 W geared dc motor through a lead screw running the length of the camera assembly. The camera which is activated remotely using an infra-red transmitter and receiver set takes pictures of isochrome patterns formed on the liquid crystal sheet.

The disk is fastened to a hollow nylon cylinder having an outside diameter of 19 cm with a wall thickness of 1.27 cm. Power to the heaters and small dc motor on the rotating disk is provided through a slip-ring-graphite-brush assembly. Copper slip rings are mounted on the nylon cylinder and graphite brushes are held in vertical brush holders. They are spring loaded to ensure constant contact with the slip rings. The nylon cylinder is housed on a steel shaft with double packed bearings for smooth operation. The complete set-up is supported on a steel platform bolted to the laboratory floor to minimize vibrational effects.

Heat is induced to the air in the test section via the heaters through a custom-designed power supply unit. Each heater is individually controlled by a variable transformer.

PROCEDURE

At the beginning of the set of test runs the liquid crystal was calibrated. A water bath was used to attain uniform isochromes on a small piece of the liquid crystal sheet used throughout this investigation. The temperature corresponding to each color was measured using a precision thermocouple and photographs were taken at laboratory conditions simultaneously so as to simulate closely the actual testing environment. The color green, corresponding to a temperature of 37°C, was chosen as the prime indicator for the temperature field. This color was easily identifiable and fluctuations in shades of green were of the order of 0.2°C.

For verification of liquid crystal accuracy, a smooth duct having

an aspect ratio of 1 and a hydraulic diameter of 3.81 cm was tested in a stationary state and compared with the well-known Dittus-Boelter (1930) correlation. Reynolds numbers were varied by changing the air mass flow rate. For each Reynolds number the heat flux was varied by changing the input voltage across the heaters. All four heaters were kept at the same power level so as to simulate a constant heat flux boundary condition. A detailed description of the data reduction process is presented in Rahman (1988). For this investigation, there existed good agreement between Nusselt numbers obtained using the liquid crystal and the Nusselt numbers predicted by the Dittus-Boelter correlation.

Each geometrical configuration was first tested in a stationary state. With the turbulators in place and fully turbulent flow conditions, the flow was hydrodynamically and thermally fully developed at the location of interest, as was seen in the periodic repetition of the isochromes on the liquid crystal sheet between each pair of turbulators at steady state conditions. For all three test sections the photographs were taken at approximately the same location, well downstream of the inlet. The area of interest was between a pair of turbulators on the heated wall. The strategy was as follows. First the Reynolds number was set by precisely fixing the mass flow rate. Heat flux was induced by switching on the power supply to the heaters. A small band of the calibrated reference color was seen immediately downstream of the left turbulator. A photograph was taken. The heater power supply was then increased so that the reference color line moved in the flow direction and another photograph was taken. This was continued until eventually the whole area between the turbulators on the heated wall was covered by the reference color at one time or another. It was observed that an average of 16 photographs were required to cover the complete area satisfactorily for a given mass flow rate. A smaller number of pictures was taken for the test section with the smallest turbulator heights and more for the test section with the largest turbulator heights. The next Reynolds number was set by changing the flow rate and the whole process was repeated, until all flow rates were tested. The same procedure was used for the other test sections.

The next step was to conduct experiments on the rotating test rig. The disk was rotated to the desired rpm and the system was allowed to come to the steady state. A picture was taken and the heat flux was increased in a manner similar to the stationary case, until a sufficient number of pictures was taken to cover the whole field. The number of pictures to be taken and the increase of heat supplied per picture was arrived at empirically. The mass flow rate was increased and another set of pictures was taken. The process was repeated for four different rpm's; 50, 100, 150 and 200. Then the direction of rotation was reversed and the whole procedure was repeated for the complete range of mass flow rates. Data acquisition was through specially written programs run on a VAX 11/785 through a dedicated IBM PC.

DATA REDUCTION

The total heat added to the air by the heaters from the inlet of the test section to the point of camera location is calculated using the formula

$$\dot{Q} = \sum_{n=1}^{k-1} i_n V_n + \left(\frac{d}{L}\right) i_k V_k - \dot{Q}_{loss} \tag{1}$$

where the camera is in front of the kth heater, d is the distance of the camera from the beginning of that heater in the flow direction, and L is the length of the heater. i_n and V_n are the current and voltage of the nth heater and $\dot{Q}_{loss}$ is the heat loss to the ambient air. The total heat is used in an energy balance equation from the test section inlet to the camera location to calculate the air mixed mean temperature at the camera location given by the following equation:

$$T_m = \frac{\dot{Q}}{\dot{m}C_p} + T_i \tag{2}$$

With T_i at about ambient temperature, T_m ranged from 24 to 28°C. The heat flux, $\dot{q''}$, for the kth heater is calculated as

$$\dot{q''} = \frac{i_k V_k}{A_h} \tag{3}$$

where A_h is the heat transfer area. The losses to the environment from the back of the heaters as well as the radiational losses from the heated surface to the unheated walls were calculated. Iterations had to be performed since the unheated wall temperature was not known a priori. The heat transfer coefficient on the turbulated side was then calculated from :

$$h_t = \frac{\dot{q''} - \dot{q_b''} - \dot{q_r''}}{(T_w - T_m)} \tag{4}$$

where T_w is the wall surface temperature and T_m is the air mixed mean temperature calculated from the energy balance mentioned above. $\dot{q_b''}$ is the heat loss through the back of the test section and

$\dot{q_r}''$ is the radiational loss from the heated wall to the three unheated walls of the test section. Substituting for the air mixed mean temperature, the expression for the heat transfer coefficient is reduced to

$$h_t = \frac{\dot{q}'' - \dot{q_b}'' - \dot{q_r}''}{T_w - T_i - \dot{Q}/(\dot{m}C_p)} \tag{5}$$

The specific heat at constant pressure, C_p, and other air properties are evaluated at the film temperature T_f which is the average of the wall surface temperature and the air mixed mean temperature.

The local Nusselt number is calculated from the formula:

$$Nu = \frac{h_t D_h}{k} \tag{6}$$

where k is the air conductivity. The above calculations were repeated for all pictures taken. The resulting data was organized into files for the appropriate test sections and runs. These results were further processed through a program to integrate these local quantities to get area weighted averages.

From observations of the liquid crystal display, in steady state conditions, it was found that the temperature patterns exhibit regular periodic behavior. For this reason only one such period, between two turbulators on the heated wall, was examined in detail and the local quantities were area-weighted over such a region. For verification, tests were repeated at two different locations from the inlet, for otherwise identical conditions, and the same results were obtained.

For all the cases, using Eq. (5), error analysis was done based on the method of Kline and McClintock (1953). Experimental uncertainties on the heat transfer coefficients are estimated to be $\pm 6\%$.

RESULTS AND DISCUSSION

The following results present data reduced for the turbulated wall. The results are reported in terms of dimensionless numbers such as Nu_r which is average Nusselt number on the turbulated wall, Re which is Reynolds number based on hydraulic diameter D_h, Rotation number, defined as $\Omega D_h/U_m$ and Rotational Reynolds Number, J_{D_h} defined as $\Omega {D_h}^2/\nu$. Reynolds number, Rotational Reynolds number and Rotation number are related as:

$$Ro = J_{D_h}/Re$$

$Gr/Re^2 = (\frac{r}{D_h})Ro^2\beta\Delta T$ ranged from 0.016 to 0.064 and the effect of centripetal buoyancy on Nusselt number was not investigated. Geometric variations are in terms of turbulator height-to-passage hydraulic diameter ratio (blockage ratio), e/D_h. The direction of rotation is taken care of by specifying the leading or trailing side of the test section. To an observer looking at the disk from the top (see Fig. 1), with the disk rotating clockwise and the heated wall on his right, then measurement is for the leading side. The wall to his left is the trailing side. If the direction of rotation is reversed, then measurements are for the trailing side. It should be noted that heat transfer coefficient is measured on the turbulated wall, but the turbulators themselves are not covered by the heaters, and hence fin type effects are not reported.

Figure 3 shows the typical variation of local Nusselt numbers in the region between two turbulators. It is seen that the heat transfer coefficient reaches a maximum where flow reattachment occurs and then decreases until the air flow approaches the next turbulator where the heat transfer coefficient increases again. This behavior is explained by the fact that after passing over the left turbulator the air flow touches the heated surface near the middle of the region thereby increasing h_t dramatically. Then as the air approaches the right turbulator a stagnation point type of situation arises with a resulting increase in heat transfer coefficient.

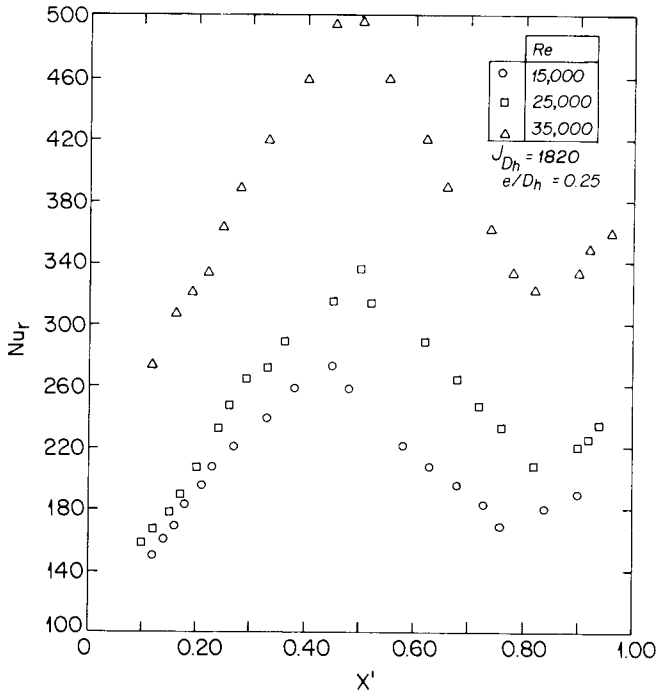

Fig. 3 Typical variation of Nusselt number between a pair of turbulators

Figure 4 shows the variation of Nusselt number for the turbulated wall with Reynolds number when the test section is stationary. These results, which are presented for the three turbulator geometries tested, are used in ensuing figures to compare the rotating versus stationary cases of otherwise identical conditions. As expected, a large increase in Nu_s is seen for test sections with higher blockage ratios over those with lower blockage ratios, due to higher level of mixing of air inside the test section.

Figures 5 through 8 show the variation of Nu_r vs Rotation number. Each figure is for a specific Rotational Reynolds number ($\Omega {D_h}^2/\nu$) i.e. a fixed value of Ω. Negative Rotation numbers imply measurements on the leading side. It is seen that Nusselt number decreases with increasing Rotation number ($\Omega D_h/U_m$) for all turbulator heights. The reason for this behavior is that, with the angular velocity Ω being fixed for each case, higher Rotation numbers correspond to lower values of U_m which in turn correspond to lower Nusselt numbers as is seen for stationary cases (see Figure 3).

Figures 9 through 11 show the variation of Nusselt number with the rotational Reynolds number for the three turbulator geometries at several Reynolds numbers. Nusselt numbers for the stationary case are shown on the $J_{D_h} = 0$ axes. It can be observed that the Nusselt number first increases as the Rotational Reynolds number (i.e. the angular velocity Ω) increases until it reaches a point of maximum and then, with the exception of the lowest Reynolds number on the trailing side, the Nusselt number decreases with J_{D_h}. This decrease is more pronounced for the smallest turbulator size. It is speculated that this behavior is due to the increase of centripetal forces with J_{D_h} which adversely affect the heat transfer coefficient in a radially outward flow. Nevertheless, compared with the stationary case, for the range of rotation numbers tested, the heat transfer coef-

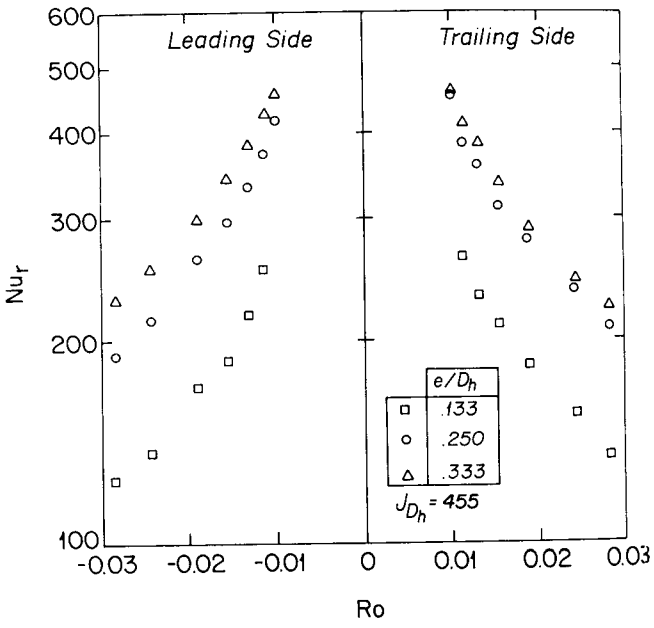

Fig. 5 Variation of Nusselt number with rotation number for three blockage ratios at a rotational Reynolds number of 455

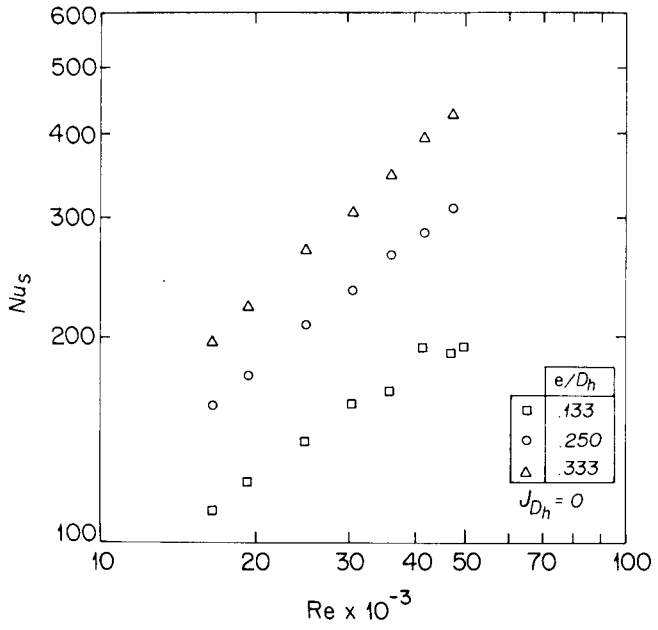

Fig. 4 Nusselt versus Reynolds number, stationary case

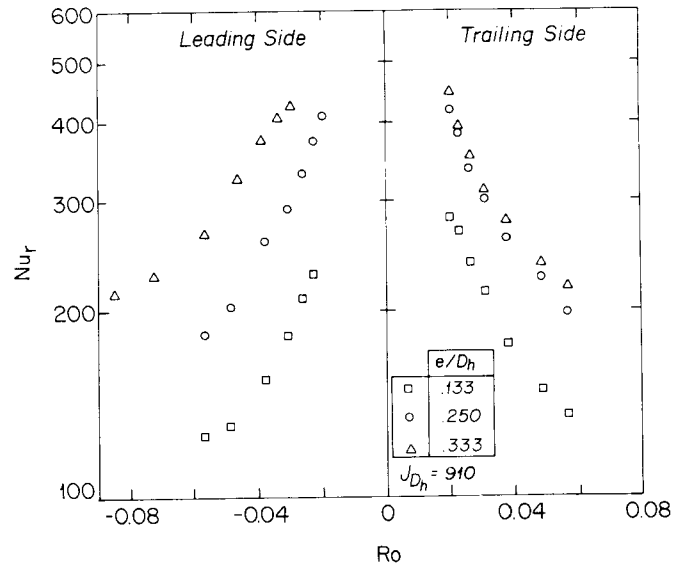

Fig. 6 Variation of Nusselt number with rotation number for three blockage ratios at a rotational Reynolds number of 910

ficient is enhanced on both leading and trailing sides for the smallest and medium height turbulators. This, however, is not the case for bigger turbulators.

A comparison between the Nusselt numbers in the stationary and rotating cases are made by plotting the ratio Nu_r/Nu_s versus Rotation number for various Rotational Reynolds numbers, as shown in Figures 12 to 14. As can be observed, rotation has a significant effect on this ratio. Large percentage increases are seen for the test sections with blockage ratios, (e/D_h), of 0.133 and 0.250.

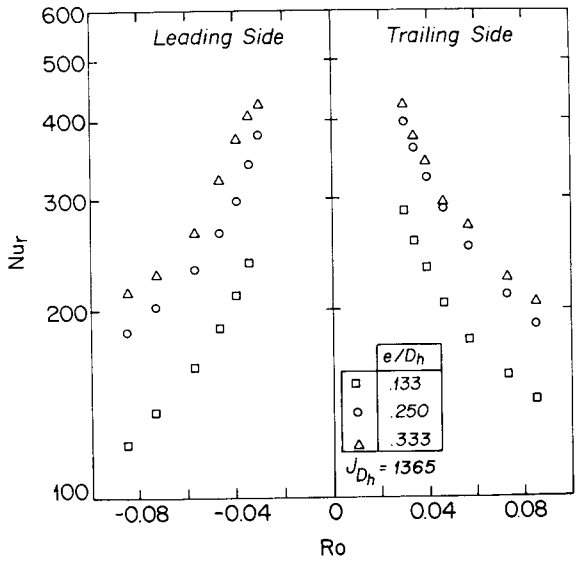

Fig. 7 Variation of Nusselt number with rotation number for three blockage ratios at a rotational Reynolds number of 1365

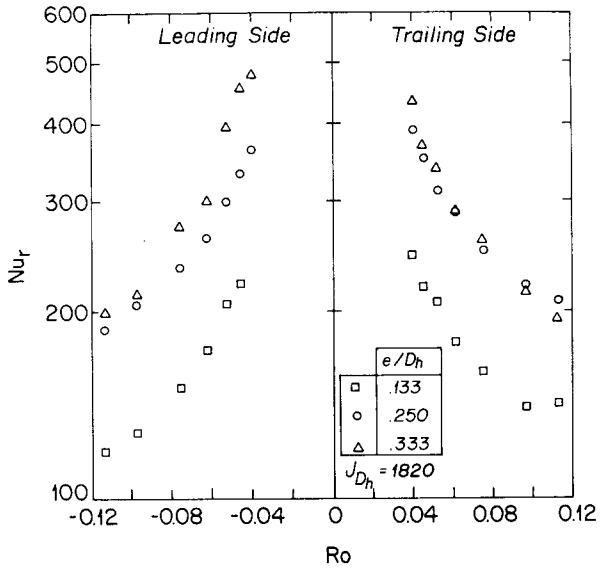

Fig. 8 Variation of Nusselt number with rotation number for three blockage ratios at a rotational Reynolds number of 1820

The least effect is for the largest size turbulators with a blockage ratio of 0.333. The maximum increase due to rotation occurs for the case of $e/D_h = 0.1333$. A 45% increase on the trailing side is seen for this blockage ratio when the Rotation number is 0.03 and J_{D_h} is 1365. The minimum occurs when the ratio Nu_r/Nu_s falls about 6% below the stationary value on the leading side for $e/D_h = 0.333$ at a Rotation number of 0.0617 and J_{D_h} of 1820. The increase for $e/D_h = 0.133$ ranges from 3% to 45%. The middle sized turbulators, with a blockage ratio of 0.250, experience an increase in the range of 11% to 40%.

The case with highest blockage ratio does not show as appreciable a change as the lowest one. Again the trend is that the ratio Nu_r/Nu_s decreases with increasing Rotational Reynolds number for the range tested.

CONCLUSIONS

Based on the experimental program described in this paper it can be concluded that : a) A significant enhancement in heat transfer is achieved both in stationary and rotating cases when the surfaces are roughened with ribs. b) For the rotating case as compared to the stationary case, a maximum increase of about 45% in the heat transfer coefficient is observed for a blockage ratio of 0.1333 and the minimum is a decrease of about 6% for a blockage ratio of 0.333, for the range of rotation numbers tested. c) The technique of using

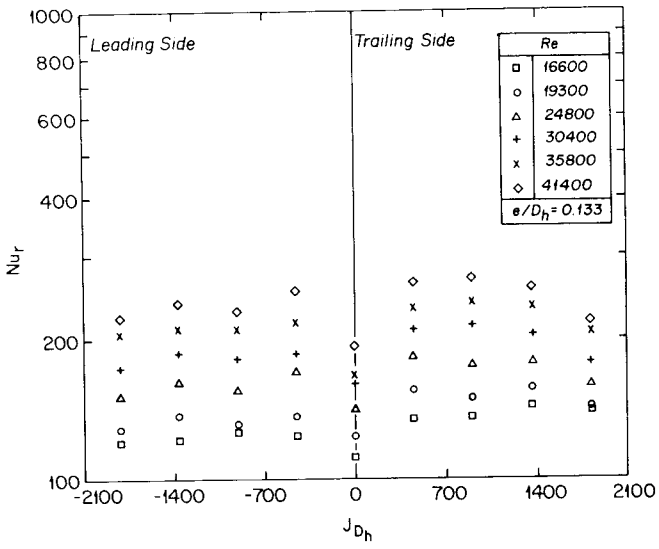

Fig. 9 Nu_r versus Rotational Reynolds number for the smallest blockage ratio

liquid crystals to determine heat transfer coefficients in this investigation proved to be an effective and accurate method, especially for rotating test sections.

ACKNOWLEDGEMENT

Financial support of The General Electric Company, Aircraft Engine Business Group, Lynn, Massachusetts is hereby gratefully acknowledged. The authors would also like to thank Mr. R.E. Gladden for his valuable suggestions during the course of this investigation.

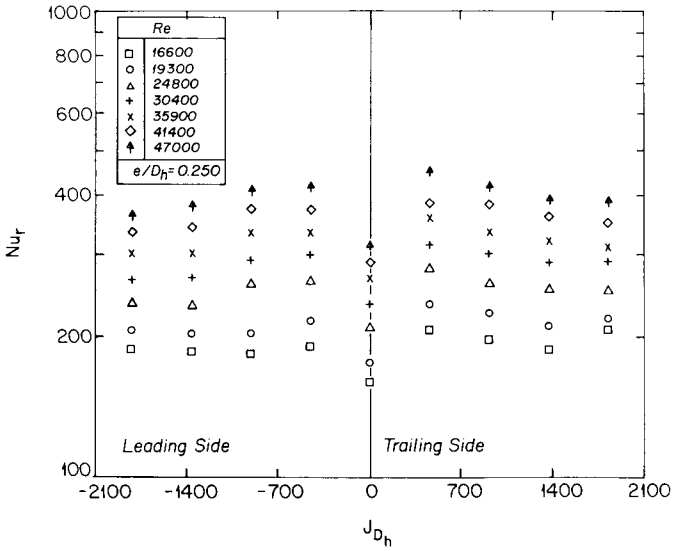

Fig. 10 Nu_r versus Rotational Reynolds number for the medium blockage ratio

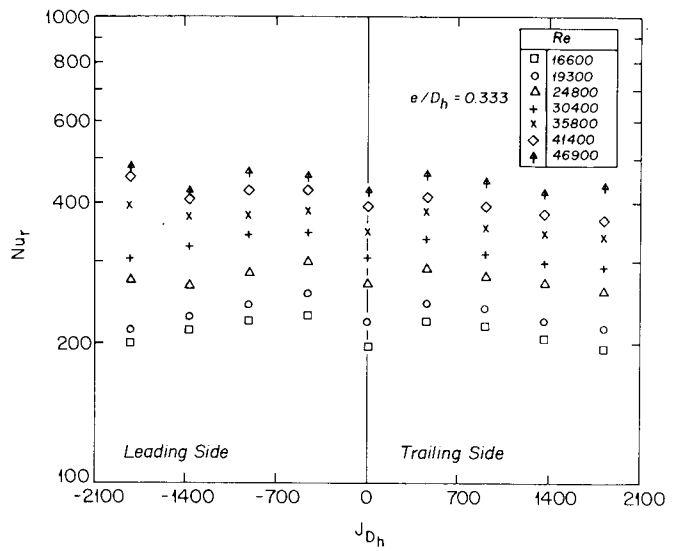

Fig. 11 Nu_r versus Rotational Reynolds number for the highest blockage retio

REFERENCES

1. Burgraff, F., 1970,"Experimental Heat Transfer and Pressure Drop with Two Dimensional Turbulence Promoters Applied to Two Opposite Walls of a Square Tube," *Augmentation of Convective Heat and Mass Transfer*, Edited by E.E Bergles and R.L. Webb, ASME, New York, pp. 70-79.
2. Han, J.C., Glicksman, L.R. and Rohsenow, W.M., 1978,"An Investigation of Heat-Transfer and Friction for Rib Roughened

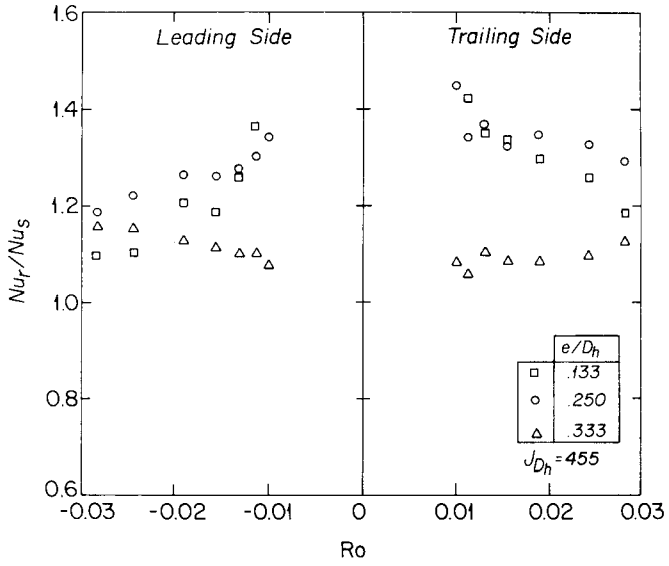

Fig. 12 Nu_r/Nu_s versus Rotation number for three blockage ratios at a rotational Reynolds number of 455

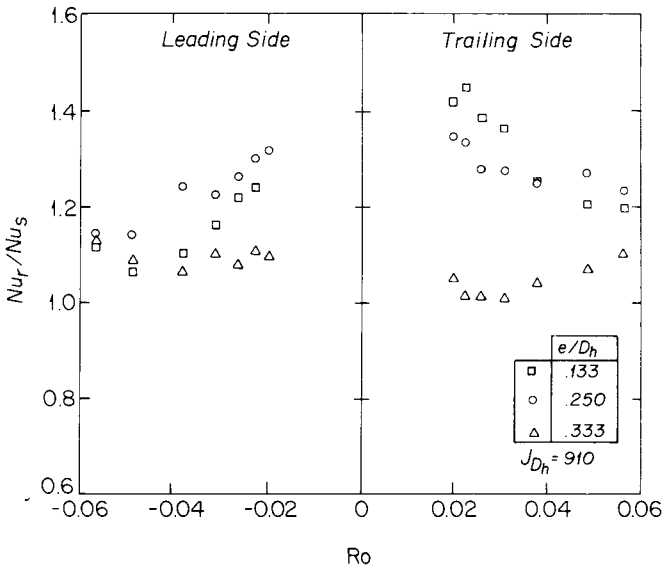

Fig. 13 Nu_r/Nu_s versus Rotation number for three blockage ratios at a rotational Reynolds number of 910

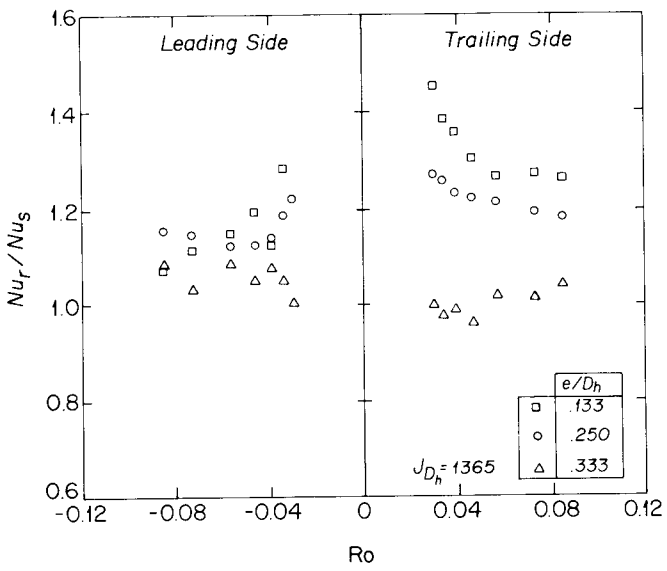

Fig. 14 Nu_r/Nu_s versus Rotation number for three blockage ratios at a rotational Reynolds number of 1365

Surfaces," *Int. J. Heat Mass Transfer*, Vol. 21, pp. 1143-1156.

3. Han, J.C., 1984," Heat Transfer and Friction in Channels with Two Opposite Rib-Roughened Walls," *ASME J. Heat Transfer*, Vol. 106, No. 4, pp. 774-781.
4. Han, J.C., Park, J.S and Lei, C.K., 1985," Heat Transfer Enhancement in Channels With Turbulence Promoters," *J. Engr. For Gas Turbines and Power*, Vol. 107, pp. 628-635.
5. Johnston, J.P., Halleen, R.M. and Lezius, D.K., 1972, " Effects of Spanwise Rotation on the Structure of Two-Dimensional Fully Developed Turbulent Channel Flow," *J. Fluid Mech.*, Vol. 56, part 3, pp. 533-557.
6. Kline, S.J., and McClintock, F.A., 1953,"Describing Uncertainty in Sigle-Sample Experiments," *Mechanical Engineering*, Vol. 75, pp. 3-8.
7. Lokai, V.I. and Limanski, A.S., 1975,"Influence of Rotation on Heat and Mass Transfer in Radial Cooling Channels of Turbine Blades," *Izvestiya VUZ, Aviatsionnaya Tekhika*, Vol. 18, No. 3, p. 69.
8. Metzger, D.E., J.W. Pennington and C.S. Fan, 1983,"Heat Transfer and Flow Friction Characteristics of Very Rough Transverse Ribbed Surfaces With and Without Pin Fins," *Proc. ASME-JSME Thermal Engineering Joint Conference*, Vol. 1, pp. 429-436.
9. Mityakov, V.Y. et al., 1978,"Turbulent Flow and Heat Transfer in Rotating Channels and Tubes," Leningrad Polytechnic Institute.
10. Mori, Y., Fukada, T. and Nakayama, W., 1971,"Convective Heat Transfer in a Rotating Radial Circular Pipe (2nd Report)," *Int. J. Heat Mass Transfer*, Vol. 14, pp. 1807-1824.
11. Morris, W.D. and Ayhan, T., 1979,"Observations on the Influence of Rotation on Heat Transfer in the Coolant Channels of Gas Turbine Rotor Blades," *Proc. Inst. Mech. Eng.*, Vol. 193, No. 21, p. 303.
12. Morris, W.D and Ayhan, T., 1981,"Heat Transfer in a Rotating Tube With Radially Inward Flow," University of Hull, Department of Engineering Design and Manufacture, Report No. EDM/4/81.
13. Morris, W.D. and Harasagama, S.P., 1987,"The Influence of Rotation on the Heat Transfer Characteristics of Circular, Triangular and Square Sectioned Coolant Passages of Gas Turbine Rotor Blades," *ASME 87-GT-121.*
14. Rahman, A., 1988,"An Experimental Investigation of Heat Transfer in a Spanwise Rotating Turbulated Passage Using Liquid Crystal Technique," *M.S. Thesis*, Mechanical Engineering Department, Northeastern University, Boston, MA 02115.
15. Taslim, M.E. and Spring, S.D., 1987,"Friction Factors and Heat Transfer Coefficients in Turbulated Cooling Passages of Different Aspect Ratios, Part I: Experimental Results," 23rd AIAA/ASME/SAE/ASEE Joint Propulsion Conference, San Diego, CA, Paper no. *AIAA-87-2009.*
16. Taslim, M.E. and Spring, S.D., 1988,"An Experimental Investigation of Heat Transfer Coefficients and Friction Factors in Passages of Different Aspect Ratios Roughened With 45° Turbulators," ASME 25th National Heat Conference, Houston, TX.
17. Taslim, M.E. and Spring, S.D., 1988,"Experimental Heat Transfer and Friction Factors in Turbulated Cooling Passages of Different Aspect Ratios, Where Turbulators are Staggered," 24th AIAA/ASME/SAE/ASEE Joint Propulsion Conference, Boston, MA, Paper no. *AIAA-88-3014.*
18. Wagner, J.H., Kim, J.C. and Johnson, B.V., 1986,"Rotating Heat Transfer Experiments With Turbine Airfoil Internal Flow Passages," *Int. Gas Turbine Conference*, 86-GT-133.
19. Zysina-Molozhen, L.M., Dergach, A.A. and Kogan, G.A., 1977," Experimental Investigation of Heat Transfer in a Radially Rotating Pipe," *HGEEE High Temp.*, Vol. 14, p. 988.